Crystallization of Isotactic Polypropylene in the Presence of a β-Nucleating Agent Based on a Trisamide of Trimesic Acid

József Varga,[1] Klaus Stoll,[2] Alfréd Menyhárd,[1,3] Zsuzsanna Horváth[1]

[1]*Laboratory of Plastics and Rubber Technology, Department of Physical Chemistry and Materials Science at Budapest University of Technology and Economics, H-1111 Budapest Mduegyetem rkp. 3. H. ép. I., Hungary*
[2]*CIBA Inc, Schwarzwaldallee 215, CH-4002 Basel*
[3]*Hungarian Academy of Sciences, Chemical Research Centre, Institute of Environmental and Material Chemistry, H-1025 Budapest, Pusztaszeri út 59-67, Hungary*

Received 16 September 2010; accepted 26 October 2010
DOI 10.1002/app.33685
Published online 3 March 2011 in Wiley Online Library (wileyonlinelibrary.com).

ABSTRACT: Tris-2,3-dimethyl-hexylamide of trimesic acid (TATA) is an new type of β-nucleating agent for isotactic polypropylene (iPP). The crystallization, melting characteristics, and the supermolecular structure of iPP nucleated with TATA were studied on the samples crystallized under nonisothermal and isothermal conditions. The β-nucleating ability of TATA was rather high even at low concentration. It was established that TATA possessed dual nucleating ability generating samples with mixed (α and β) polymorphic compositions. The β-content showed an maximum value at low concentrations (10–100 ppm) of TATA. The β-content decreased with increasing concentration of TATA in the higher concentration range. The highest β-content (about 80%) was achieved at the crystallization temperature T_c = 110–120°C at low concentration of TATA. The crystallization curves registered at constant cooling rate or under isothermal condition have a single peak in spite of the formation of two polymorphic modifications. The crystallization isotherms cannot be linearized according to the Avrami equation because of simultaneous crystallization of the α-and β-forms, having different nucleation and growth rate. It was also found that the β-content increased with increasing conversion during isothermal crystallization because of the higher growth rate of the β-phase. The β-phase formed in the presence of TATA consist of lamellar crystallites. In the early stage of the crystallization, hedritic structure is formed. © 2011 Wiley Periodicals, Inc. J Appl Polym Sci 121: 1469–1480, 2011

Key words: β-nucleating agent; calorimetry; crystallization; isotactic polypropylene; melting; supermolecular structure

INTRODUCTION

Semicrystalline isotactic polypropylene (iPP) is a polymorphic material with different modifications including the monoclinic (α), trigonal (β), and orthorhombic (γ) forms.[1,2] In the last two decades, the β-modification of iPP (β-iPP) has been studied intensively. β-iPP seems to be a complementary type of the traditional α-form now. For the preparation of iPP products rich in the β-form or pure β-iPP, the addition of the selective β-nucleating agents (β-NA) is the most feasible method.[1] The first highly active β-NA was the γ-modification of linear *trans*-quinacridone (LTQ), introduced by Leugering.[3] Two-component β-NA based on calcium stearate and pimelic acid was proposed by Shi et al.[4] Varga et al.[5] have found that calcium salts of pimelic and suberic acid are highly thermostable β-NA, which is selective exclusively to the β-form. In the presence of latter, pure β-iPP could be prepared. A commercial type of β-NA is *N*,*N*′-dicyclohexyl-2,6-naphthalene-dicarboxamide under the trade name NJS NU100.[6–12] On the contrary to the common artificial nucleating agents, it is partially soluble in iPP melt.[10–12] An other commercial β-NA of aryl amide type with undisclosed chemical structure is TMB-5.[13] To trigger the formation of β-iPP, one can use derivatives of terephthalamide,[14,15] glutaramide,[16] succinamide,[17] and adipamide[18] as well. Recently, Dou and Lu[19–21] have found that some metallic salts of malonic acid possess β-nucleating ability. Some complexes of rare earth metal (denoted as WBG) can also induce the formation of the β-form.[22–24] Recently, Zhang et al.[25] and Yang et al.[26] showed that the mixture of nano-$CaCO_3$ and pimelic acid can be used as a two-component β-NA. It is worth mentioning that there are several other β-NA-s with low or moderate β-nucleating ability.[1]

In the recent years, trisamides of trimesic acid were discovered and widely investigated as a very stable and highly versatile class of nucleating

Correspondence to: A. Menyhárd (amenyhard@mail.bme.hu).

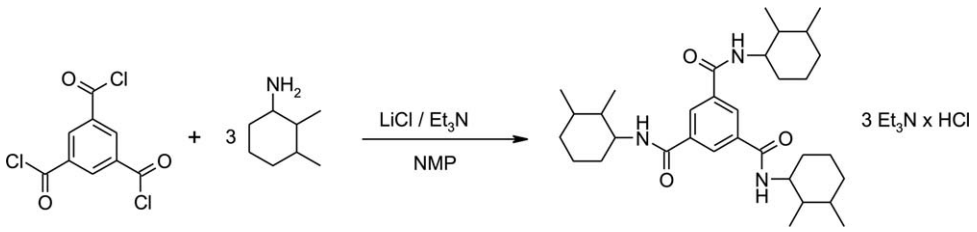

Scheme 1 The synthesis reaction of TATA.

agents.[27] Distinct structural variations allow to design nucleators and clarifiers with various properties. They may be extraordinary efficient at low concentrations (few hundred ppm and even less). Developed for the common α-form of iPP, the first trisamide clarifier was commercially introduced by Ciba. in 2006 [c.f. WO 04/072168]. It was recognized, however, that members of aromatic trisamides family may work as β-NA for iPP [c.f. WO 03/102069]. The effects of various β-NA-s on the melting and crystallization behavior of iPP were previously compared and already published elsewhere.[10]

Our preliminary results included first findings with one experimental trisamide from Ciba (designated as CG-220), which has been studied more in detail and is now reported herein. Further aim of this work is to introduce the methodology of qualifying a β-NA, because lot of contradictory works is presented in the literature in this field. The major problem is that several authors do not take into account the unique melting behavior of beta nucleated iPP,[1,28] and the results obtained in those works do not represent the polymorphic composition of the samples reliably.[29–32] Moreover, it was also highlighted in this work that β- and α-iPP crystallize simultaneously during isothermal crystallization study, and therefore the Avrami evaluation of crystallization isotherms recorded by DSC is fundamentally flawed, because the crystallization process of the two modifications is impossible to separate. Despite that several paper is dealing with the kinetic evaluation of β-nucleated iPP according to Avrami method.[23,33] The competitive growth of the two phase can only be studied by Wide angle X-ray scattering (WAXS) technique presented by Chen et al.[34]

MATERIALS AND METHODS

Experimental

Materials

Tipplen H-890 polypropylene homopolymer (MFR = 0.35 dg/min at 230°C, 2.16 kg) was used in this study as received from TVK Hungary. The β-NA being a trisamide of trimesic acid (TATA) was prepared according to the following procedure (see in Scheme 1):

About 36.5 g (0,284 mol) 2,3-dimethyl-cyclohexylamine, 2.8 g (0,066 mol) lithium chloride, 35.5 g (0.344 mol) triethyl-amine, and 130 mL NMP were placed in a 500-mL three-necked flask. About 26.6 g (0.086 mol) 1,3,5-benzene-tricarboxylic acid trichloride dissolved in 50 mL NMP were added to this clear yellow solution at 5°C over a period of 1 h. After stirring for 2 h at 75–80°C, the reaction mixture was chilled and poured under stirring into 600-mL ice water. The precipitate was filtered off, then washed with 200 mL water and 400-mL hot methanol, and eventually dried in a vacuum oven at 80°C. About 33 g of 1,3,5-benzene-tricarboxylic acid tris(2,3-dimethyl-cyclohexylamide) was finally obtained (71% yield) as faintly yellowish powder with a melting point >300°C. *Elemental analysis:* Calculated values for $C_{33}H_{51}N_3O_3$: C 73.70%; H 9.56%; N 7.81%; experimentally determined values: C 73.33%; H 9.51%; N 7.87%. TATA is thermally stable compound, and its intensive thermal degradation in inert atmosphere occurs above 400°C (Fig. 1). The nucleating agent crystallizes in needle form (Fig. 2).

Methods

IPP samples with TATA content of 10, 50, 100, 300, 500, and 1000 ppm were prepared in a Brabender

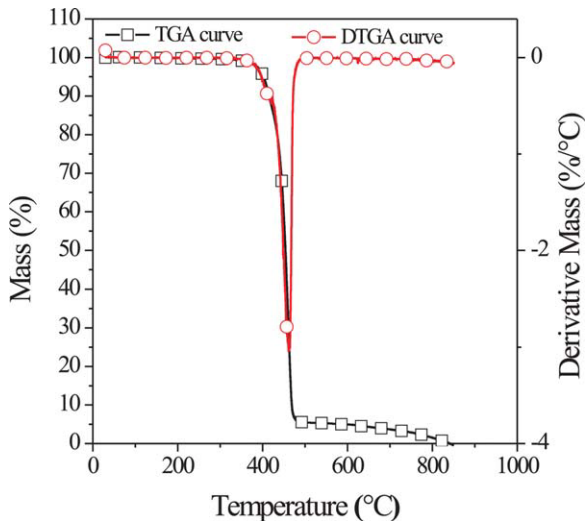

Figure 1 Thermogravimetric (TG) trace of TATA. [Color figure can be viewed in the online issue, which is available at wileyonlinelibrary.com.]

Figure 2 SEM micrographs of the TATA crystals.

W 50 internal mixer at 220°C and 50 rpm. The β-nucleated samples were crystallized under nonisothermal and isothermal conditions. The crystallization and melting characteristics and polymorphic composition were determined with a Perkin–Elmer DSC-7 calorimeter applying cooling rates (V_c) of 10°C/min and at varied heating (V_h) rates. For erasing the thermal and mechanical history, the samples were heated up to 220°C and held there for 5 min. To determinate of the real polymorphic content based on the calorimetric melting curves, the disturbing effect of βα-recrystallization occurring during heating of samples cooled to the room temperature was eliminated. As we demonstrated,[1,28,35] the β-phase melts without βα-recrystallization if it is not cooled below the critical temperature $T_R^* \approx 100$°C. Therefore, the end temperature of cooling (T_R) was set to $T_R^* = 100$°C during nonisothermal crystallization (limited recooling). The samples crystallized isothermally were heated up from T_c. The features of βα-recrystallization were studied on samples, cooled to 25°C, and heated with different heating rates. For studying of the βα-recrystallization, the temperature-modulated DSC (TMDSC) is useful method, because it permits to separate of the melting and recrystallization processes.[1,10,36] The TMDSC traces of the samples crystallized at a cooling rate of $V_c = 10$°C/min were recorded with an Universal V4.0B TA Instrument at $V_h = 2$°C/min, with modulation ± 0.3°C and 50 s.[10]

The supermolecular structure of the samples was studied by polarized light microscopy (PLM) and scanning electron microscopy (SEM). The PLM investigations were carried out on a Leitz Dialux 20 optical microscope equipped by a Polaroid DMC Model 1 digital camera and the micrographs were recorded by Image Pro Plus software. The samples were melted during PLM studies using a Mettler FP82HT hot stage. To determine the optical character of the samples studied, a λ-plate located diagonally between the crossed polarizers was used. The samples were crystallized under isothermal conditions after the elimination of thermal and mechanical history by heat treatment of the samples at 220°C for 5 min. The samples were cooled to various crystallization temperatures (T_c) at a rate of 5 C/min or quenched (uncontrolled cooling to T_c as fast as possible), and the structure formed during these isothermal experiments was studied by PLM.

SEM micrographs were taken from selected samples using JEOL JSM 6340LA type equipment with an electron acceleration voltage of 23 kV. The samples were prepared using a Mettler FP82HT hot stage. They were melted at 220°C, and the thermal and mechanical prehistory was erased at 220°C for 5 min. Then the samples were quenched to $T_c = 130$°C and held there until they completely crystallized. The surface of the samples was etched with a permanganate solution (5 mL) for 6 h according to the method introduced by Olley and Bassett.[37] WAXS patterns were recorded with a Philips PW 1830/PW type equipment with Cu Kα radiation at 40 kV and 35 mA. The scanning rate was 2°/min.

Determination of the nucleation ability of the beta-nucleating agents

The nucleating *ability* of β-NAs could be characterized by their *selectivity* and *efficiency*.[10] The *selectivity* of the β-NAs is quantified by the β-content of the samples. For the determination of the relative β-content, Turner Jones et al.[38] introduced the k value, which can be calculated according to Eq. (1) on the basis of the diffractogram recorded by WAXS measurements:

$$k = \frac{H_{\beta 1}}{H_{\beta 1} + (H_{\alpha 1} + H_{\alpha 2} + H_{\alpha 3})} \tag{1}$$

where $H_{\alpha 1}$, $H_{\alpha 2}$, and $H_{\alpha 3}$ are intensities of α-diffraction peaks corresponding to angles $2\theta = 14.2°$, 17.0°, and 18.4°, respectively, $H_{\beta 1}$ is the intensity of β-diffraction peak corresponding to angle $2\theta = 16.2°$. The k value is a relative measure to assess the polymorphic composition but numerically does not express the absolute value of β-content (β_c), although its value is 0 for α-IPP and 1 for β-iPP as it is apparent.

The β-content can be determined on the basis of the calorimetric melting curves of the samples with mixed polymorphic composition as well. As we emphasize earlier, *the calorimetric method based on the evaluation of the melting curves gives reliable results, if the beta to alpha recrystallization is eliminated*. The β-content can be determined according to the Eq. (2)[39]:

$$\beta_c = \frac{X_\beta}{X_\beta + X_\alpha} = \frac{\frac{\Delta H_\beta}{\Delta H_\beta^0}}{\frac{\Delta H_\beta}{\Delta H_\beta^0} + \frac{\Delta H_\alpha}{\Delta H_\alpha^0}} \tag{2}$$

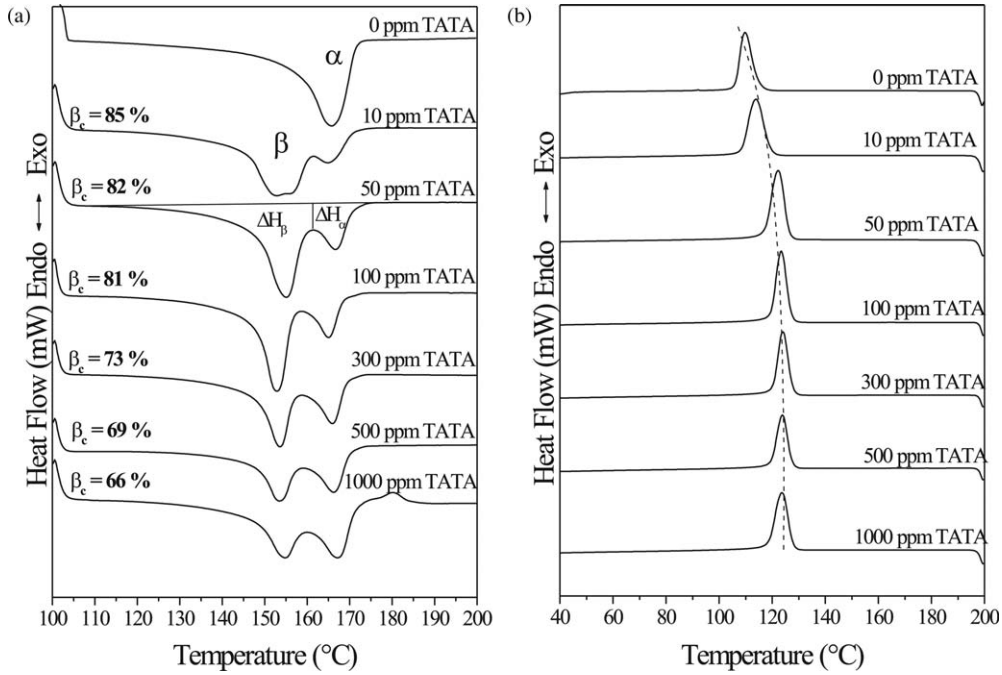

Figure 3 Effect of the concentration of TATA on the melting (a) and crystallization (b) curves of the nucleated samples. Cooling and heating rate $V_c = V_h = 10°C\ min^{-1}$, $T_R = T_R^* = 100°C$).

where the β_c is the β-content, X_β and X_α are the degree of crystallinity of the α- and β-form, respectively, and ΔH_α^0 and ΔH_β^0 are the enthalpy of fusion of the completely crystallized α- and β-forms, while ΔH_α and ΔH_β the enthalpy of the fusion of the α- and β-forms in the samples with mixed polymorphic composition. ΔH_α and ΔH_β can be determined from the area under α- and β-melting peaks. Unfortunately, the literature values for the enthalpy of fusion of α- and β-iPP are rather contradictory[1,40] and strongly depend on the method of their determination. There are three pairs of enthalpy values determined by similar method.[1] These are the following for the α- and β-form: 170.0 and 168.5 J/g,[41] 221 and 192 J/g,[42] and 148 and 113 J/g,[43,44] respectively. In spite of the notable difference in numerical values of the enthalpy of fusion determined by different methods, the β_c differs only slightly applying the above values in Eq. (2), because the determining factor is the quotient $q = \Delta H_\alpha^0/\Delta H_\beta^0$ and not the absolute value of the enthalpy according to the Eq. (2):

$$\beta_c = \frac{q}{q + \frac{\Delta H_\alpha}{\Delta H_\beta}} \tag{3}$$

The Eq. (3) is obtained after introducing q in Eq. (2).

In most of cases, the α- and β-melting peaks are overlapped, and thus they should be separated. The simplest approximation of the partition is the drawing a vertical line through the maxima between the two endothermic peaks.[45] The low temperature part of area gives ΔH_β and the high temperature area corresponds to ΔH_α [see Fig. 3(a)]. To take into the account the degree of overlapping of the α- and β-melting peaks, Li and Cheung[29] proposed an empirical equation with a correction factor (C_f). Unfortunately, they evaluated the melting curves of the β-nucleated samples cooled to 50°C when concluding of their equation. Consequently, the disturbing effect of the βα-recrystallization was not eliminated. Therefore, the reliability of the proposed equation seems to be questionable, although this method was already applied in several woks. We separate the melting peaks by the method of the vertical line[38] using the following equilibrium enthalpy values of fusion: $\Delta H_\alpha^0 = 148\ J/g$[43] and $\Delta H_\beta^0 = 113\ J/g$.[44]

The nucleating efficiency of the additives can be characterized by their influence on the peak temperature of the crystallization curves (T_{cp}) registered at a constant cooling rate during nonisothermal crystallization. It is worth of mentioning that Lotz and colleagues[46] proposed an efficiency scale, which is based on the comparison of the peak temperature of the crystallization of non-nucleated (T_{c1}), nucleated (T_{cNA}), and self-seeded (T_{c2}) samples according to the Eq. (4):

$$NE = \frac{T_{cNA} - T_{c1}}{T_{c2}} \times 100\% \tag{4}$$

where T_{cNA}, T_{c1}, and T_{c2} are the peak temperatures of the nucleated non-nucleated and self-seeded samples, respectively. Unfortunately, this equation cannot be adopted for β-iPP, because the β-nucleated

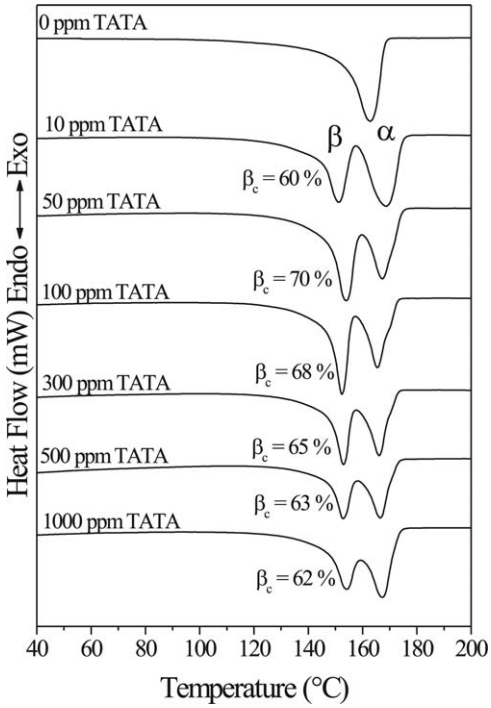

Figure 4 Effect of the concentration of TATA on the melting curves of the recooled samples (heating rate $V_h = 10°C$ min^{-1}, recooling temperature $T_R = 25°C$).

samples heated slightly above the melting point of the β-phase $T_m(\beta)$ recrystallize always in the α-modification.[47] Therefore, the determination of T_{c2} is impossible. Consequently, we characterize the efficiency of the β-NAs simply by T_{cp} recorded during nonisothermal crystallization at a cooling rate of 10°C.

RESULTS AND DISCUSSION

Nonisothermal crystallization

The melting curves of the nonrecooled ($T_R = 100°C$) samples containing different amount of TATA after nonisothermal crystallization are shown in Figure 3(a). The corresponding crystallization curves are seen in Figure 3(b). For comparison purpose, the melting curves of recooled samples ($T_R = 25°C$) are presented in Figure 4. The evaluation of the melting curves of nonrecooled samples, which reflect the real polymorphic composition, proves that the nucleated samples are rich in the β-form, in fact. This is manifested in the pronounced melting peaks located in the temperature range of 150–155°C. The high temperature peaks observed at about 165°C correspond to the melting of the α-phase. Accordingly, samples with mixed polymorphic composition are formed in the presence of TATA. As a consequence, TATA has dual nucleating ability. The β-content has a maximum value at very low concentration (10–100 ppm) of TATA, and it decreases with increasing concentration of the nucleating agent in

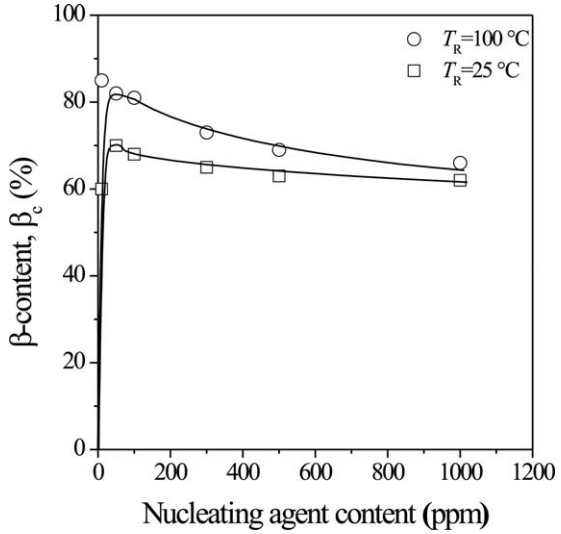

Figure 5 Dependence of the β-content (β_c) of nonrecooled and recooled samples on the concentration of TATA.

the higher concentration range. It is worth to notice that in the presence of calcium suberate, being a completely selective β-NA, the β-content is increased monotonously with increasing concentration before reaching a saturation value at high concentration.[5] The β-content of the recooled and nonrecooled samples as a function of TATA concentration is shown in Figure 5. It is clearly seen that the β-content of

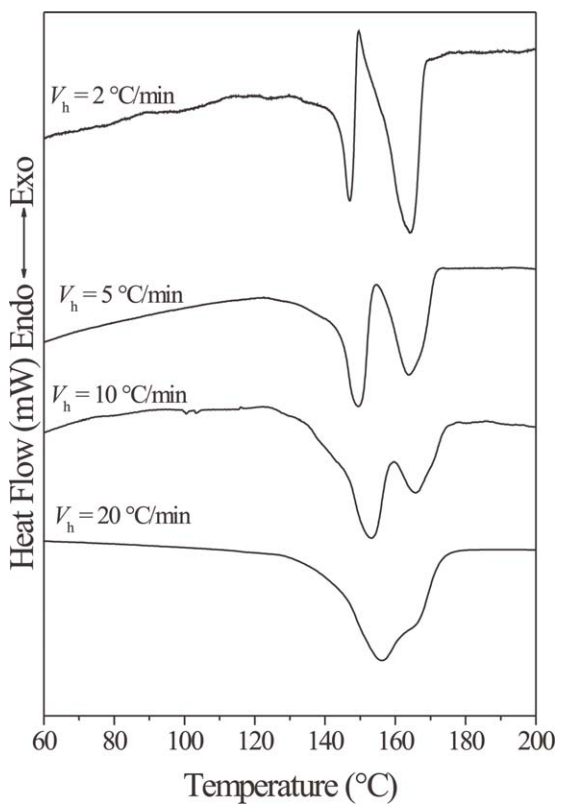

Figure 6 Effect of the heating rate on the melting profile of beta nucleated sample containing 50 ppm of TATA.

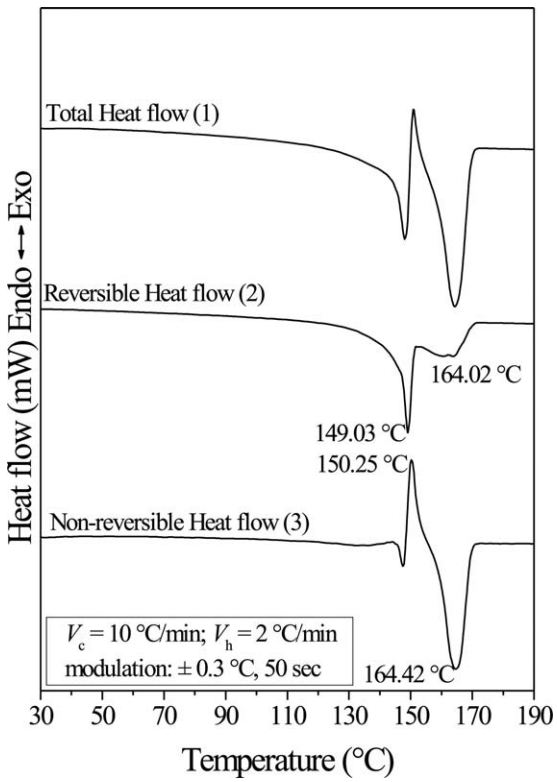

Figure 7 TMDSC curves of β-nucleated sample containing 100 ppm TATA.

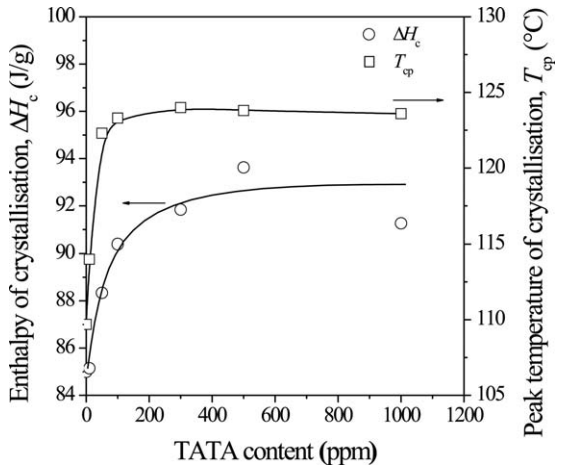

Figure 8 Dependence of the enthalpy (ΔH_c) and peak temperature of crystallization (T_{cp}) on the concentration of TATA.

nonrecooled samples is always higher. It should be emphasized that the β_c of recooled samples is an apparent value. The reduction of β_c in recooled samples is the consequence of the formation of the α-phase during heating of recooled samples undergoing βα-recrystallization. The α-melting peaks of recooled samples have a shoulder at high temperature, which indicates for two crystal fraction of the α-phase (See in Figure 4). The first one is the α-phase formed during the primary crystallization, whereas the second one is due to the beta to alpha recrystallization during heating. The latter fraction melts at higher temperature because of its formation (recrystallization) at higher temperature. This was suggested by the high temperature shoulder. The alpha to beta recrystallization is a time-dependent process. Therefore, the melting profile and the relative intensity of α- and β-melting peaks, and, consequently, the calculated apparent β-content of the recooled samples strongly depends on the heating rate. Lowering the heating rate promotes the recrystallization. Hence, the α-melting peak became more intensive and the β-melting peak decreased simultaneously (Fig. 6). According to MDSC measurements, the beta to alpha recrystallization occurs during the partial melting of the β-phase (Fig. 7). The nonreversible heat flow traces indicate that the irreversible exothermic recrystallization is superimposed on the reversible melting of the β-phase. The temperature lag between reversible melting of β-phase and the irreversible βα-recrystallization is very small (about 1°C), that is, the melted β-phase immediately recrystallizes into the α-phase (Fig. 7). This phenomenon is characteristic for the β-phase in general and independent on the nature and concentration of the β-NA-s.[10]

The above-discussed results prove once again that the calorimetric determination of the β-content based on the melting curves of recooled samples is not

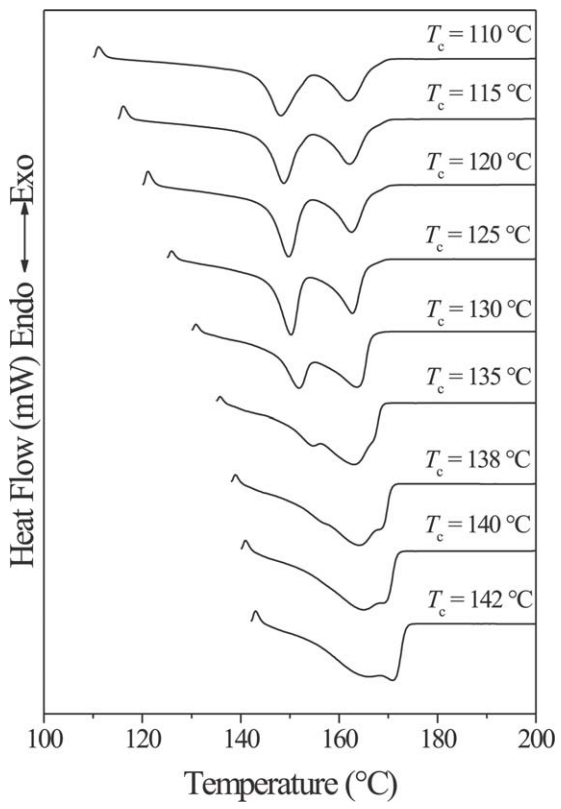

Figure 9 Melting curves of isothermally crystallized sample containing 1000 ppm of TATA.

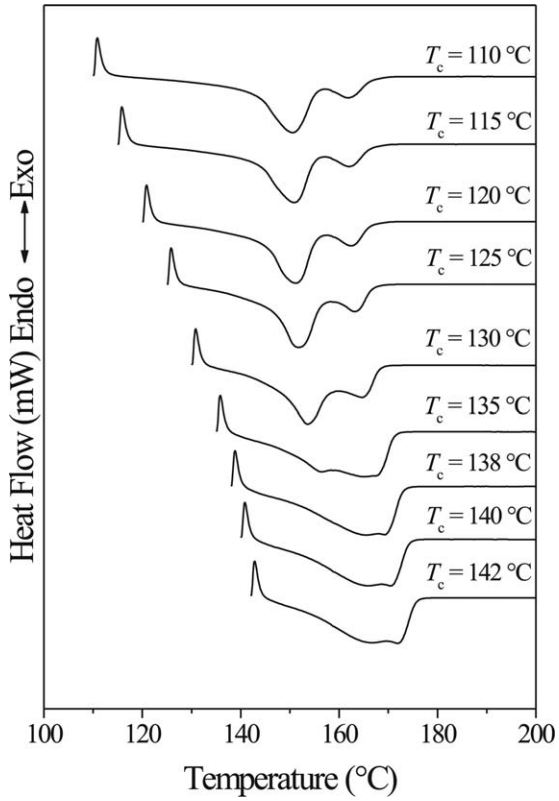

Figure 10 Melting curves of isothermally crystallized sample containing 100 ppm of TATA.

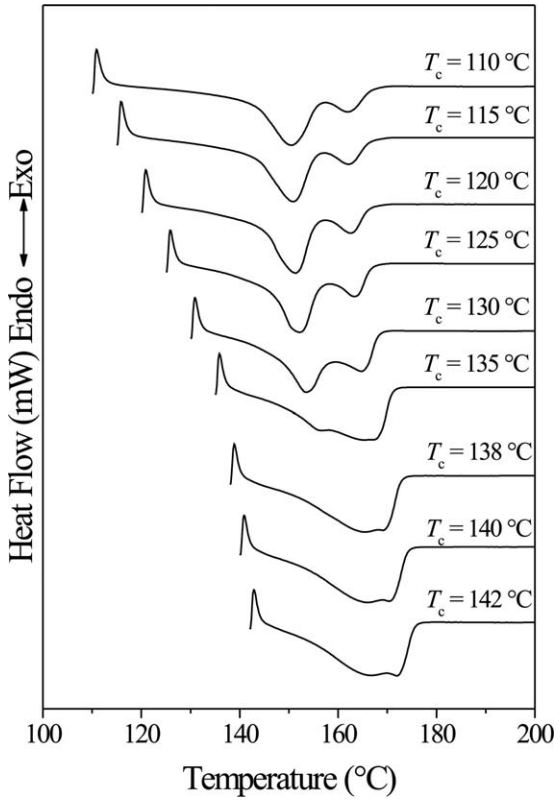

Figure 11 Melting curves of isothermally crystallized sample containing 50 ppm of TATA.

reliable because of the disturbing effect of the alpha to beta recrystallization. Therefore, the literature data obtained in this way should be treated with criticisms.

The crystallization curves of β-nucleated samples show only single peaks [Fig. 3(b)] in spite of the formation of two different polymorphs existing as individual, separate phases. In accordance with the nucleating ability of TATA, the temperature range and peak temperature of the crystallization (T_{cp}) are shifted toward higher temperatures with increasing concentration of the nucleating agent. The dependence of the peak temperature (T_{cp}) and the enthalpy (ΔH_c) of crystallization on the concentration of the TATA are displayed in Figure 8. The increasing of ΔH_c with increasing concentration of TATA could be explained with increasing α-content having higher enthalpy of fusion. Moreover, the crystallinity becomes larger because of elevating the crystallization temperature with increasing the TATA concentration.

Isothermal crystallization

The isothermal crystallization of the β-nucleated samples with different TATA concentration was performed in the temperature range T_c = 110–145°C. Melting curves of samples heated from T_c without recooling are shown in Figures 9–11. The β-content as a function of T_c for the samples with different TATA concentrations is shown in Figure 12. In the temperature range 110–135°C, the samples are rich in β-modification. The highest β_c (about 80%) can be achieved at lower crystallization temperatures (T_c = 110–125°C) with 10–100 ppm TATA concentration. Above T_c = 135°C, the β-phase forms only in

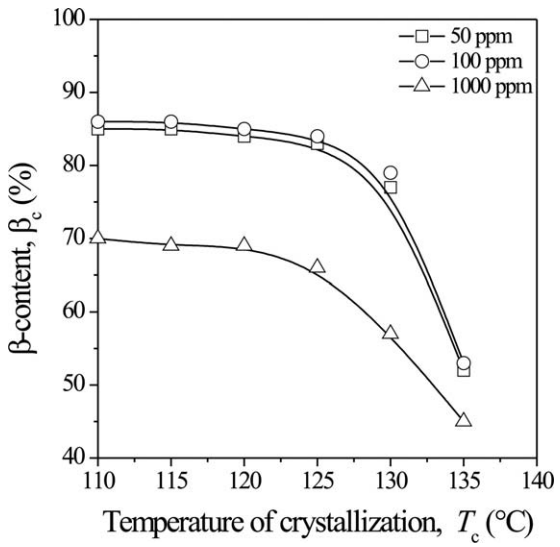

Figure 12 Dependence of the β-content on the temperature of the isothermal crystallization and concentration of TATA.

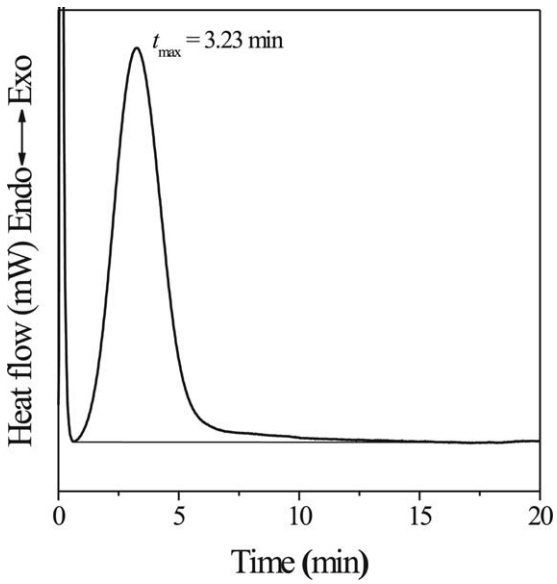

Figure 13 Crystallization isotherm of sample containing 100 ppm TATA at $T_c = 130°C$.

traces, if any (Figs. 9–11). The double-melting peaks of the α-modification formed in β-nucleated samples above 135°C similar to those of α-iPP reported first by Samuels.[48] This α-peak duplication is connected with the α_2 to α_1 recrystallization.[40,49,50]

The crystallization isotherms monitored at different T_c for the samples containing 1000, 100, and 50 ppm TATA show single peaks (Fig. 13) in spite of the formation of both α- and β-modifications. This indicates that the formation of two polymorphs occurs simultaneously. At low T_c ($T_c < 125°C$), the crystallization occurs partially during the cooling to T_c. Hence, the early stage of the crystallization cannot be evaluated exactly. At high T_c, the samples

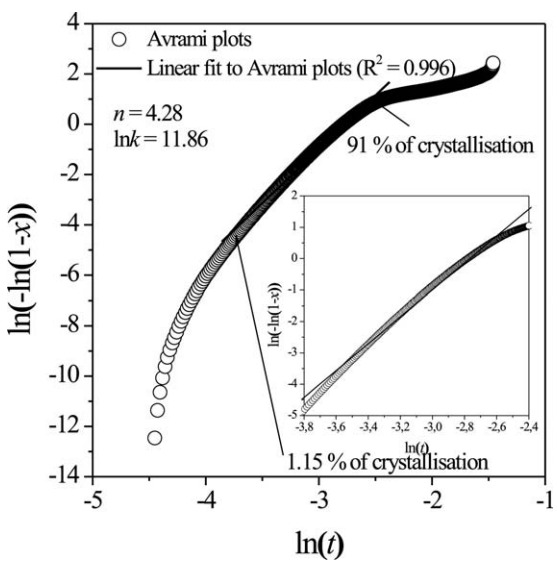

Figure 14 Evaluation of crystallization isotherms according to the Avrami equation.

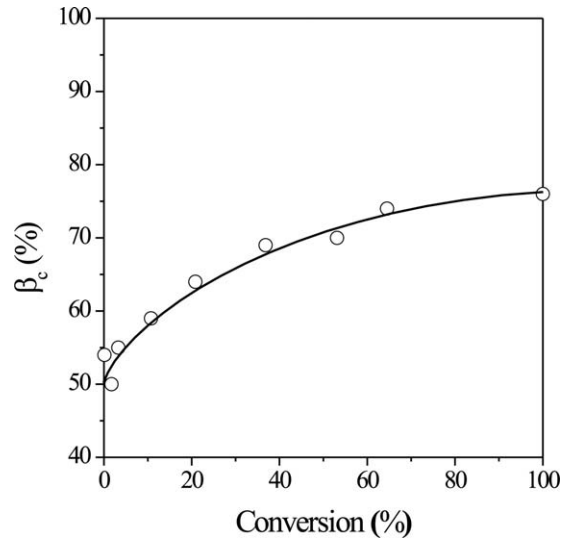

Figure 15 The change of β_c during isothermal crystallization at 130°C (concentration of TATA: 1000 ppm, heating started from T_c).

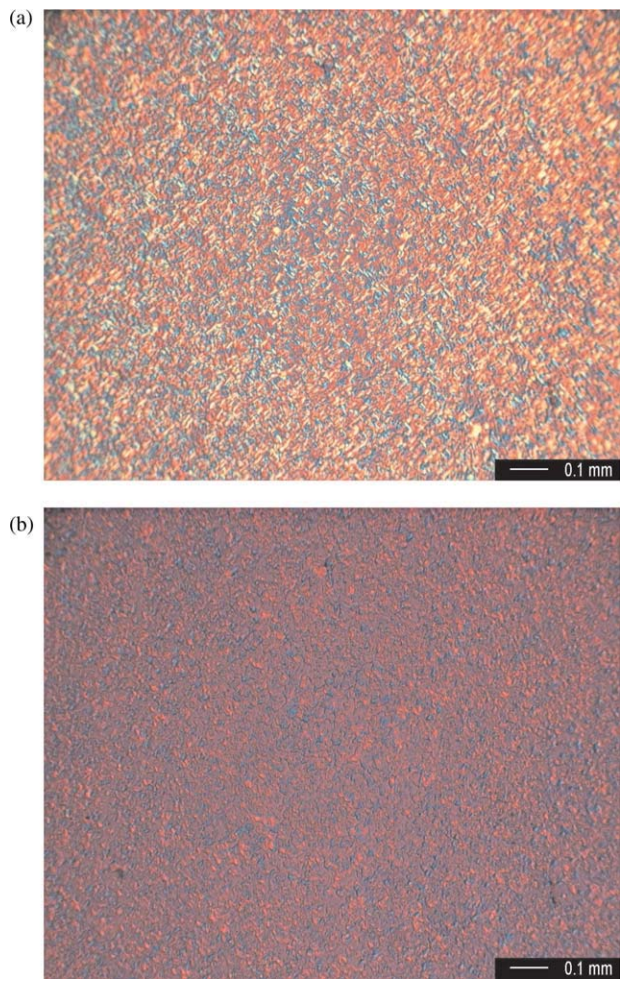

Figure 16 Microcrystalline structure of the sample crystallised at a cooling rate $V_c = 10°C$ containing 1000 ppm (a) and the α-phase remaining after selective melting of β-iPP at $T = 155°C$ (b). Heating started from T_c, concentration of TATA: 1000 ppm. [Color figure can be viewed in the online issue, which is available at wileyonlinelibrary.com.]

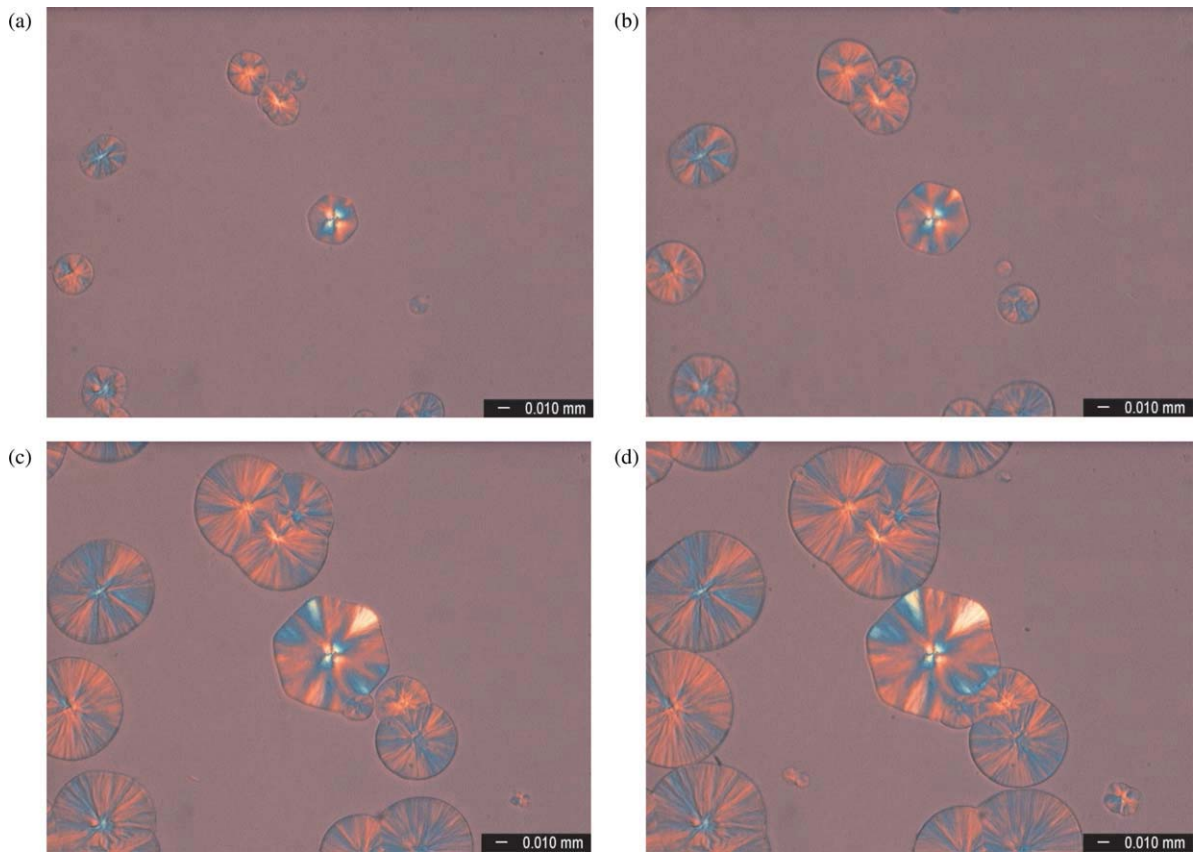

Figure 17 Formation a β-hexagonite (in the center) during isothermal crystallization of sample containing 10 ppm TATA (T_c = 135°C, t_c = 22, 30, 45, and 50 min). [Color figure can be viewed in the online issue, which is available at wileyonlinelibrary.com.]

crystallize slowly. Therefore, the crystallization isotherms are rather flat, and it is difficult to mark out the base line. Isotherms, suitable for the quantitative evaluation, are available only in a narrow temperature range (T_c = 125–130°C). The crystallization isotherms registered in this temperature range were evaluated by the Avrami equation:

$$x = 1 - e^{kt^n} \quad \text{or} \quad \ln(-\ln(1-x)) = n\ln t + \ln K \quad (5)$$

where K is the rate constant of the crystallization, n is the Avrami's exponent, and x is the relative proportion of crystallized material. However, the crystallization isotherms of the samples nucleated with TATA could not be linearized by the Avrami equation (Fig. 14). It is clearly visible in Figure 14 that Avrami plots have no linear section in the whole crystallization range. A linear line was fitted to Avrami plots in the conversion range of 1.15–91%. We have to remark here that the correct estimation of the initial time (t_0) of crystallization is essential. If the line is fitted to a small section of the Avrami plots, the fitting might be good, but the results obtained will not be reliable. Avrami plots presented in Figure 14 indicate unambiguously that the n depends on time due to the crystallization of the α- and β-forms with different nucleation and growth rate occurs simultaneously. This scenario results in very complicated overall process. One can only speculate how the overall rate of the crystallization and the polymorphic composition depend on the crystallization time or conversion under isothermal condition. In the presence of β-NA with dual nucleating ability, it is most probable that the nucleation of the α- and β-phase is athermal (i.e., the number of the nuclei of both phases are constant during the crystallization). In this case, the polymorphic composition is determined by the relative growth rate of the polymorphs and the relative number of the athermal α- and β-nuclei. It is known that the growth rate of the β-phase is higher than that of the α-phase in the temperature range T = 100–140°C,[1,40] and the ratio of the growth rate is temperature dependent. Consequently, the β-content assumed to be increased with increasing crystallization time or conversion. The experimental results corroborate the above assumption. The alteration of β_c of the samples as a function of the conversion during the isothermal crystallization is demonstrated in Figure 15. The samples were crystallized isothermally at 130°C for different times and than heated from T_c. β_c was determined on the basis of the melting curve as described earlier [see eqs. (2)

and (3)]. It is well seen that in the initial stage of the crystallization TATA induces the formation of α- and β-phase nearly in equal extent ($\beta_c \approx 0.5$). This suggests a similar nucleating activity of TATA in relation to the β- and α-forms. The β-content increased monotonously with the conversion because of the higher growth rate of the β-phase, as supposed (Fig. 15). Because the relative growth rate and the selectivity of the nucleating agent are temperature dependent the quantitative description of the crystallization kinetics induced by nucleating agent with dual nucleating ability is rather complex and it is unresolved as yet. Therefore, the published kinetic characteristics (K, n) determined from the evaluation of the crystallization isotherms registered in the presence of nonselective β-NA should be treated with criticism.

Supermolecular structure of samples nucleated TATA

In most of the publications addressing the beta nucleated iPP, the supermolecular structures of the samples are displayed in their final appearance similar to the micrograph showed in Figure 16(a). This micrograph demonstrates that microcrystalline structures with high birefringence are developed, confirming the presence of the β-form. The structure remaining after the separate melting of the β-phase [Fig. 16(b)] reveals that notable amount of the α-phase was also present.

There are only few papers giving a detailed study of developing the supermolecular structures of iPP in the presence of β-NA. In one of our previous papers, it was demonstrated with PLM and SEM that hedritic crystallization takes place in the early stage of the crystallization in the presence of highly selective calcium pimelate and calcium suberate.[1,51,52] The hedrites are polygonal formations consisting of lamellar crystallites. The β-hedrites lying flat on have hexagonal shape (hexagonite), but the hedrites edge on, are seen as rodlike formation according the PLM micrographs. The hedrites overgrow into the spherulites in the later stage of the crystallization. On the contrary, the transcrystallization plays essential role in the structure developing in presence of certain β-NA-s like NJ Stars and TMB-5.[11,13,14] The β-phase forms as a transcrystalline overgrowth on the surface of the needlelike crystals of these β-NA-s recrystallized from the iPP melt.[11,13]

The open question is how the β-NA of aromatic trisamid type influences the feature of the supermolecular architecture of β-form. For its better understanding, we studied the crystallization by PLM at high T_c in the vicinity of upper temperature of the formation of the β-phase[1,40] at very low concentration of the nucleator. Under this condition, the β-content is low, but the early stage of the β-crystal growth can be followed continuously on optical level. It was found that hedrites are also formed in the early stage of the crystallization in the presence of TATA. In Figure 17, the growth of a well-developed β-hedrite laying flat on (hexagonite) is shown. The banded β-spherulite located in the center of the PLM micrographs (Fig. 18) was developed from a β-hedrite standing edge on. These observations suggest that the supermolecular structure in the presence of TATA develops in similar manner as in the presence of calcium pimelate and suberate. Some SEM micrographs taken from etched surface of the isothermally crystallized sample are shown in Figure 19. The β-phase formed in the presence of TATA consists of lamellar crystallites arranged in stacks. Most of the β-lamellae are also seen edge on [Fig. 19(a,b)], but in some region of the sample lamellae laying flat on are discernible. In Figure 19(c,d), we show regions containing both edge on and flat on β-lamellae and lamellae tilted from the plane sample. On the surface of lamellae, flat on etching pits is observable indicating the presence of

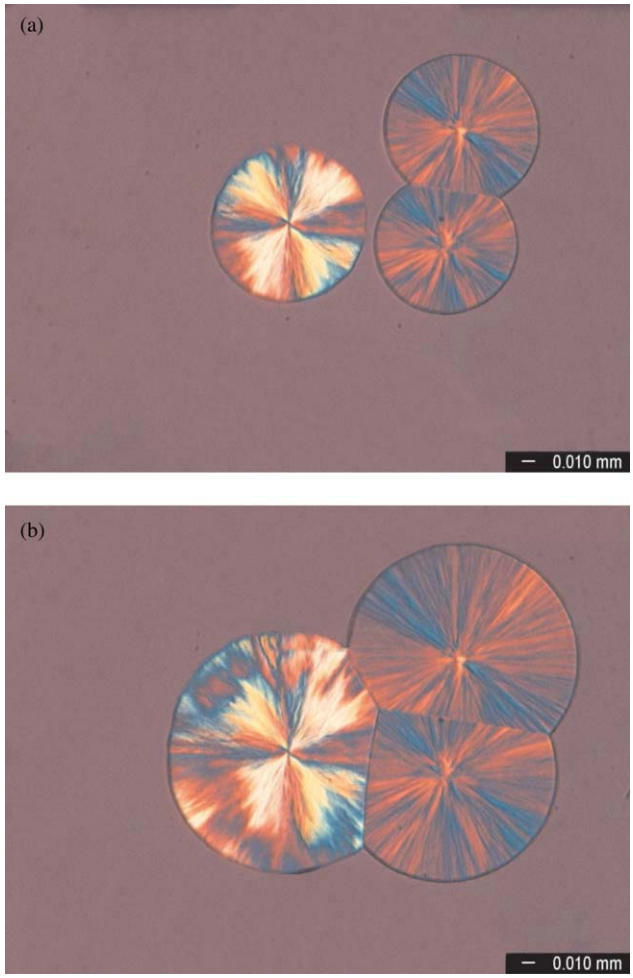

Figure 18 Formation of a banded β-spherulite during isothermal crystallization of sample containing 10 ppm TATA ($T_c = 138°C$, $t_c = 60$ and 90 min). [Color figure can be viewed in the online issue, which is available at wileyonlinelibrary.com.]

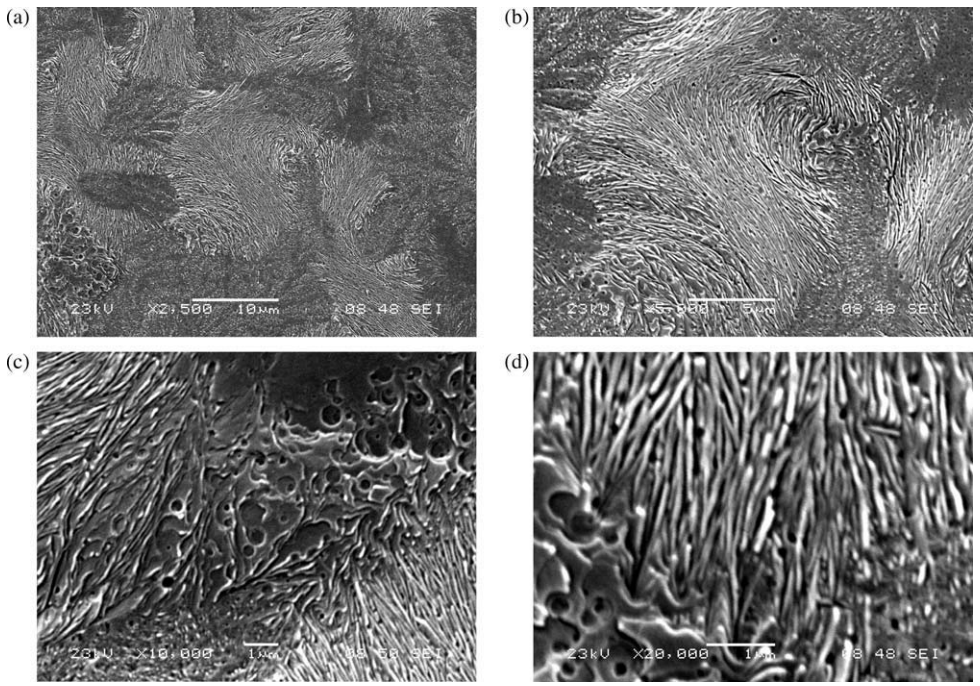

Figure 19 Arrangement of the β-lamellae in the sample nucleated with 100 ppm TATA and crystallized at $T_c = 130°C$ for 30 min.

spiral dislocations, which are responsible for lamellar branching.[1,51,52]

CONCLUSIONS

TATA is an active β-NA. In its presence, samples with mixed polymorphic compositions form, which indicates that TATA possesses dual nucleating ability. The β-content has maximum value at low concentration (10–100 ppm) of TATA. During isothermal crystallization, the highest β-content (about 80%) can be achieved at lower crystallization temperatures ($T_c = 110–125°C$) at 10–100 ppm TATA concentrations. The crystallization curves registered at constant cooling rate or under isothermal condition have a single peak in spite of the formation of two polymorphic modifications. The crystallization isotherms cannot be linearized according to the Avrami equation because of the simultaneous crystallization of the α-and β-forms, having different nucleation and growth rates. It was also found that the β-content increased with increasing conversion during isothermal crystallization because of the higher growth rate of the β-phase. The β-phase formed in the presence of TATA consists of lamellar crystallites. In the early stage of the crystallization, a hedritic structure is formed.

References

1. Varga, J. J Macromol Sci Phys 2002, B41, 1121.
2. Lotz, B.; Wittmann, J. C.; Lovinger, A. J Polym 1996, 37, 4979.
3. Leugering, H. J. J Macromol Chem 1967, 109, 204.
4. Shi, G. Y.; Zhang, X. D.; Qiu, Z. X. Makromol Chem 1992, 193, 583.
5. Varga, J.; Mudra, I.; Ehrenstein, G. W. J Appl Polym Sci 1999, 74, 2357.
6. Ikeda, N.; Kobayashi, T.; Killough, L. Novel beta-nucleator for polypropylene; Polypropylene '96. World Congress, Zürich, Switzerland, 1996.
7. Marco, C.; Gomez, M. A.; Ellis, G.; Arribas, J. M. J Appl Polym Sci 2002, 86, 531.
8. Kotek, J.; Raab, M.; Baldrian, J.; Grellmann, W. J Appl Polym Sci 2002, 85, 1174.
9. Cermak, R.; Obadal, M.; Ponizil, P.; Polaskova, M.; Stoklasa, K.; Lengalova, A. Eur Polym J 2005, 41, 1838.
10. Menyhárd, A.; Varga, J.; Molnár, G. J Therm Anal Calorim 2006, 83, 625.
11. Varga, J. Menyhárd, A. Macromolecules 2007, 40, 2422.
12. Behrendt, N.; Mohmeyer, N.; Hillenbrand, J.; Klaiber, M.; Zhang, X. Q.; Sessler, G. M.; Schmidt, H. W.; Altstadt, V. J Appl Polym Sci 2006, 99, 650.
13. Dong, M.; Guo, Z.; Yu, J.; Su, Z. J Polym Sci B 2008, 46, 1725.
14. Mathieu, C.; Thierry, A.; Wittmann, J. C.; Lotz, B. J Polym Sci Part B: Polym Phys 2002, 40, 2504.
15. Mohmeyer, N.; Schmidt, H. W.; Kristiansen, P. M.; Altstadt, V. Macromolecules 2006, 39, 5760.
16. Lu, Q.; Dou, Q. e-Polymers 2008, 076.
17. Lu, Q. L.; Dou, Q. J Macromol Sci Part B: Phys 2008, 47, 463.
18. Dou, Q. J Appl Polym Sci 2009, 111, 1738.
19. Dou, Q.; Lu, Q. L. J Vinyl Addit Technol 2008, 14, 136.
20. Dou, Q.; Lu, Q. L.; Li, H. D. J Macromol Sci Part B: Phys 2008, 47, 900.
21. Dou, Q.; Lu, Q. Polym Adv Technol 2008, 19, 1522.
22. Xiong, F.; Guan, R.; Xiao, Z. X.; Xiang, B. L.; and Lu, D. P. Polym Plast Technol Eng 2007, 46, 97.
23. Xiao, W.; Wu, P.; Feng, J. J Appl Polym Sci 2008, 108, 3370.
24. Xiao, W. C.; Wu, P. Y.; Feng, J. C.; Ya, R. Y. J Appl Polym Sci 2009, 111, 1076.
25. Zhang, Z.; Wang, C.; Yang, Z.; Chen, C.; Mai, K. Polymer 2008, 49, 5137.

26. Yang, Z.; Zhang, Z.; Tao, Y.; Mai, K. Eur Polym J 2008, 44, 3754.
27. Blomenhofer, M.; Ganzleben, S.; Hanft, D.; Schmidt, H.-W.; Kristiansen, M.; Smith, P.; Stoll, K.; Mader, D.; Hoffmann, K. Macromolecules 2005, 38, 3688.
28. Varga, J. J Therm Anal 1986, 31, 165.
29. Li, J.; Cheung, W. J Therm Anal Calorim 2000, 61, 757.
30. Liu, M. X.; Guo, B. C.; Du, M. L.; Chen, F.; Jia, D. M. Polymer 2009, 50, 3022.
31. Tang, X. G.; Yang, W.; Bao, R. Y.; Shan, G. F.; Xie, B. H.; Yang, M. B.; Hou, M. Polymer 2009, 50, 4122.
32. Kang, J.; Chen, J. Y.; Cao, Y.; Li, H. L. Polymer 2010, 51, 249.
33. Zhao, S.; Cai, Z.; Xin, Z. Polymer 2008, 49, 2745.
34. Chen, Y. H.; Mao, Y. M.; Li, Z. M.; Hsiao, B. S. Macromolecules 2010, 43, 6760.
35. Varga, J. J Therm Anal 1989, 35, 1891.
36. Karger-Kocsis, J.; Shang, P. P. J Therm Anal 1998, 51, 237.
37. Olley, R. H.; Bassett, D. C. Polymer 1982, 23, 1707.
38. Turner Jones, A.; Aizlewood, J. M.; Beckett, D. R. Macromol Chem 1964, 75, 134.
39. Shangguan, Y. G.; Song, Y. H.; Peng, M.; Li, B. P.; Zheng, Q. Eur Polym J 2005, 41, 1766.
40. Varga, J. In Crystallization, Melting and Supermolecular Structure of Isotactic Polypropylene; Karger-Kocsis, J., Ed.; Chapman & Hall: Netherlands, 1995; p 56.
41. Li, J. X.; Cheung, W. L.; Jia, D. M. Polymer 1999, 40, 1219.
42. Shi, G. Y.; Huang, B.; Zhang, J. Y. Makromol Chem Rapid Commun 1984, 5, 573.
43. Monasse, B.; Haudin, J. M. Colloid Polym Sci 1985, 263, 822.
44. Varga, J; Garzó, G. Acta Chim Hungar 1991, 128, 303.
45. Li, J. X.; Cheung, W. L. J Mater Process Technol 1997, 63, 472.
46. Fillon, B.; Lotz, B.; Thierry, A.; Wittmann, J. C. J Polym Sci Part B: Polym Phys 1993, 31, 1395.
47. Varga, J.; Schulek-Tóth, F.; Ille, A. Colloid Polym Sci 1991, 269, 655.
48. Samuels, R. J. J Polym Sci Part B: Polym Phys 1975, 13, 1417.
49. Petraccone, V.; Derosa, C.; Guerra, G.; Tuzi, A. Makromol Chem Rapid Commun 1984, 5, 631.
50. Derosa, C.; Guerra, G.; Napolitano, R.; Petraccone, V.; Pirozzi, B. Eur Polym J 1984, 20, 937.
51. Varga, J.; Ehrenstein, G. W. Colloid Polym Sci 1997, 275, 511.
52. Trifonova-Van Haeringen, D.; Varga, J.; Ehrenstein, G. W.; Vancso, G. J. J Polym Sci Part B: Polym Phys 2000, 38, 672.